Is the world running out of fresh water?

By TAMMA CARLETON, LEVI CREWS, AND ISHAN NATH*

PRELIMINARY AND INCOMPLETE DRAFT - JANUARY 2024

Systematic global assessments of the world's evolving water resources have been an expanding area of work in the scientific literature in recent years (e.g., Rodell et al., 2018), but have thus far received little attention in economics. While the total quantity of water contained within the earth and its atmosphere is fixed over time, the water available *for human consumption* can evolve dynamically. Indeed, Tapley et al. (2019) estimate that recent decades have seen a substantial transfer of water mass from land, where most water is fresh and usable by humans, to the oceans, which are generally prohibitively expensive to desalinate for human use.

Even within the earth's land area, the welfare consequences of water resource depletion can differ substantially across space. Declining water availability is more likely to be harmful in regions that are highly populated, have low existing water resources, and are highly specialized or especially productive in agriculture, which is by far humanity's most water-intensive endeavor. Existing scientific literature has raised a range of concerns about the implications of trends in water resources for topics of first order importance in economics, including threats to global food supplies (Gleick and Cooley, 2021), and the role of global markets in mediating local water depletion (Dalin et al., 2017).

In this paper, we leverage a newly assembled collection of globally comprehensive geospatial and remotely sensed data from Carleton, Crews and Nath (2023) to establish a set of stylized facts about the evolution of water resources in recent decades and its potential implications for human welfare. We restrict our attention to arable land, given that agriculture accounts for $\sim$90% of human water use (Mekonnen and Hoekstra, 2011). We show that, on average, global arable land is *not* losing water resources over time.[1] Almost exactly equal shares of the world's arable land are losing and gaining water over the last two decades, and the net change in total water volume is almost exactly zero.

However, while there is no overall net trend in water available for global agriculture, some regions are experiencing rapid water loss that may be cause for concern. We show that the parts of the world losing water fastest are home to a disproportionate share of the world's population and exhibit low average rainfall and surface water availability. Reassuringly, these rapidly depleting regions have the least conducive soil and climate conditions for agriculture of any arable land on Earth, though they are farmed intensively enough to account for a substantial share of current global agricultural production.

Finally, we investigate the role of global trade in mediating the consequences of local water scarcity by computing global water use embedded in international agricultural shipments. We show that "virtual water" imports flow into some of the water-scarcest regions, preventing further water depletion. The contribution of this paper is limited to these descriptive facts, but we emphasize that recent advances in data availability and the pressing importance of this topic presents a range of opportunities for future work in economics on open questions about global policy, international trade, water resources, and welfare.

I. Global Trends in Fresh Water Resources

For much of human history, global data on water resources was limited to a patchwork collection of observations from wells and gauges

* Carleton: University of California, Santa Barbara, Bren School of Environmental Science & Management (email: tcarleton@ucsb.edu); Crews: Princeton University, Department of Economics (email: lcrews@princeton.edu); Nath: Federal Reserve Bank of San Francisco (email: inath33@gmail.com). We thank Cheikh Fall and Christian Hilgemann for excellent research assistance, Maren Ludwig and Dylan Hogan for sharing code and materials, Adrien Bilal for helpful comments, and the Global Commission on the Economics of Water for support. Any views in this paper are those of the authors and do not necessarily reflect those of the Federal Reserve System.

[1] Stable water supplies on arable land can be reconciled with large transfers of water from land to the oceans by evidence that the latter is dominated by melting ice from mountain ranges and glaciers (Chen, Wilson and Tapley, 2013).

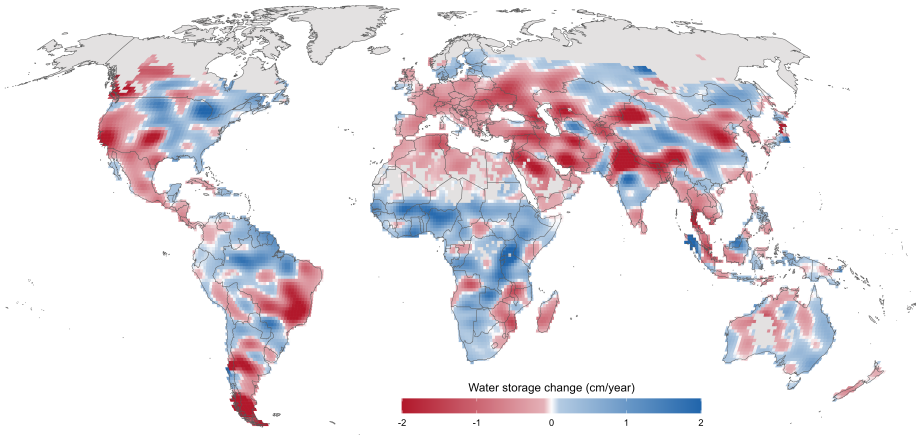

FIGURE 1. TRENDS IN TOTAL WATER STORAGE OVER ARABLE LANDS

Note: Annual changes in total water storage (TWS) over arable land during the Gravity Recovery and Climate Experiment (GRACE) satellite record (2003-2022). Colors indicate the linear trend in TWS (in centimeters of equivalent water height per year) for each $\sim 1^\circ$ equal-area grid cell. Trends are estimated via grid-specific regressions including monthly fixed effects. GRACE data are derived from the Goddard Space Flight Center (available here). All regions in grey indicate non-arable land.

measuring groundwater, rivers, and rainfall, all of which suffered from inconsistent geographic and temporal coverage. In recent decades, remote sensing has enabled scientists to quantify water resources with unprecedented scale and scope. Perhaps most importantly, the Gravity Recovery and Climate Experiment (GRACE) uses satellite measurements of small changes in the earth's gravitational pull at each grid cell to provide a monthly measure of local changes in "total water storage" (ΔTWS), defined as the aggregate volume of water in a location, including groundwater, soil moisture, surface water, snow, and ice (Tapley et al., 2004). A substantial body of scientific literature validates the water volume interpretation of GRACE data, and also highlights important measurement limitations. We discuss these further in Appendix A.A.

Figure 1 plots the trend in TWS recovered by GRACE over the satellite record period of 2003-2022 for all arable land at the level of equal-area grid cells that measure $1^\circ \times 1^\circ$at the equator. We define arable land as any GRACE grid cell containing either cropped area or pasture land as estimated by Monfreda, Ramankutty and Foley (2008). The data show tremendous heterogeneity throughout the world, at both regional scales—with broad patterns of loss or gain across regions such as Europe and the Middle East—and at more local scales—with diverging subnational patterns within countries such as the U.S., India, and Australia.

We calculate that water losses and gains on arable land are in near perfect balance. Over the satellite record, 51.2% of arable acreage lost water, while 48.8% gained. Total losses slightly exceeded total gains, such that global arable land lost 105 km^3 per year, or 9 m^3/ha per year. For context, this rate of net loss amounts to 0.1% of average annual rainfall on arable land, or 1.2% of the estimated total water used in global crop production (see Appendix A.B).

Note that this paper does not examine the relative contributions of various natural and anthropogenic factors driving observed trends, nor do we infer whether they are likely to continue in the future. Each of these topics is the subject of a growing scientific literature.

II. Regional Trends and Existing Scarcity

While water resources on arable land appear to be stable on average in recent decades, Figure 1 shows substantial losses in many regions. To the extent that the marginal value of water depends on its scarcity, such declines are likely to be most consequential for welfare in locations with low baseline water availability. To investigate the correlation between water losses and water scarcity, Figure 2a and Appendix Figure A1 map changes in total water storage

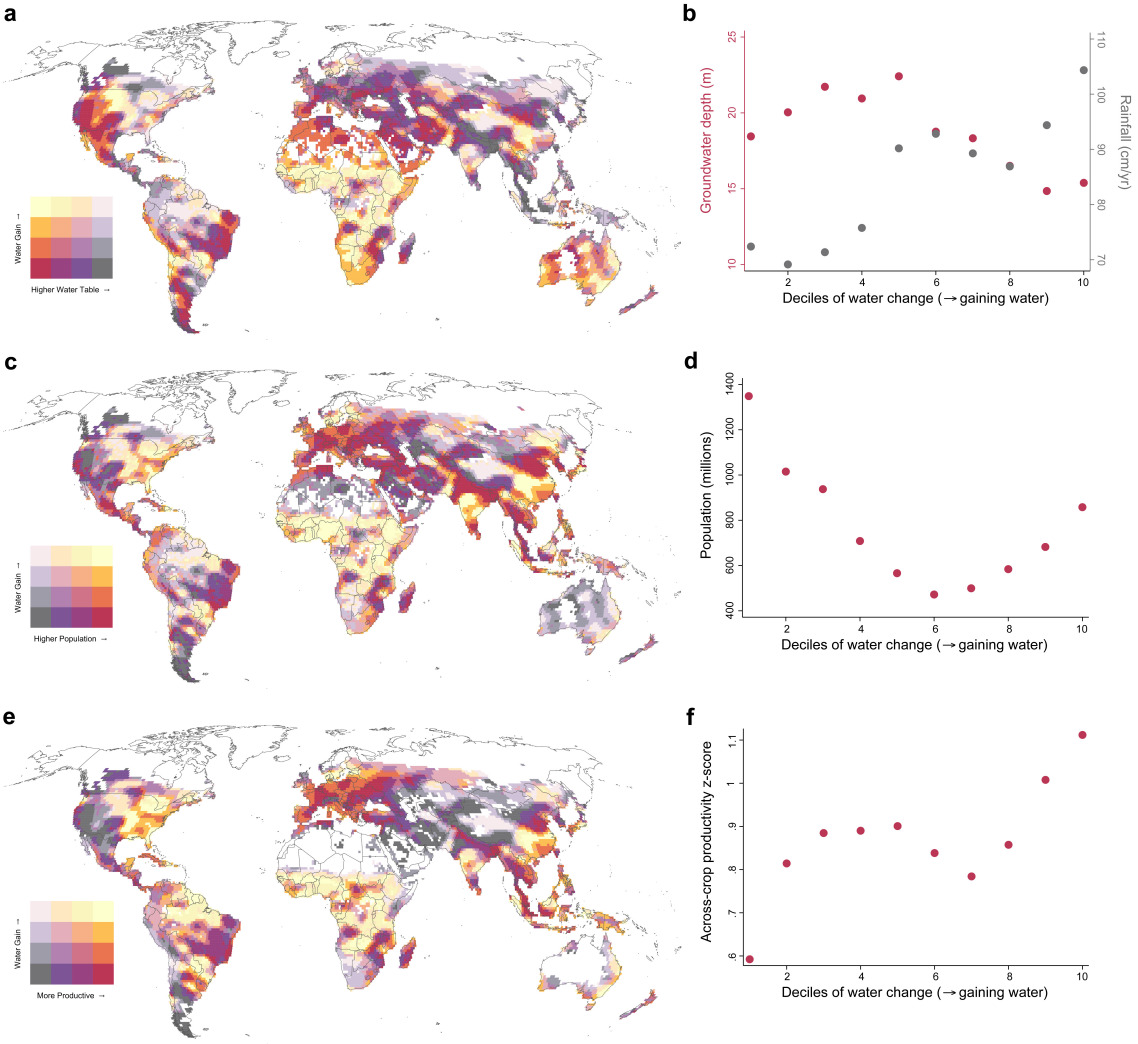

FIGURE 2. ECONOMIC CORRELATES OF WATER LOSS AND GAIN ON ARABLE LAND

Note: Maps show trends in total water storage from Figure 1 against: **a,** depth to groundwater from Fan, Li and Miguez-Macho (2013); **c,** total population from the Global Human Settlement Layer produced by the European Commission; and **e,** average agricultural productivity, assembled from GAEZ. Scatter plots show the following variables for each decile of total water storage trends: **b,** average depth to groundwater (pink) and average annual rainfall from the European Centre for Medium-Range Weather Forecasts Reanalysis v5 (grey); **d,** total population; and **f,** average across-crop agronomic productivity.

against gridded estimates of groundwater table depth, rainfall, and surface water prevalence. The corresponding graphs to the right of each map plot each of these measures of water availability against deciles of trends in ΔTWS across global arable land on the *x*-axis. For context, regions in the leftmost decile are depleting water each year at a rate equivalent to 2-5% of the amount needed to grow barley, a relatively low water-intensity crop, on each arable hectare.

Together, the figures show some evidence that regions suffering rapid water declines are those that are already water scarce. Regions losing water fastest are those with the lowest annual average rainfall and prevalence of lakes, rivers, and streams. The pattern for groundwater table depth is more nuanced. Regions with the lowest water tables (furthest from the surface, and thus least easily accessible) are losing water on average, but the most extreme water losses are concentrated in places with average water table depth. Overall, we calculate that just 6.8% of the world's arable land is in the bottom quartile of both groundwater availability and trends

in water resources. These regions with low existing stocks and rapid depletion, which include large parts of the Middle East, the southwestern United States, northern China, eastern Brazil, and southern Argentina, are likely those that suggest the greatest cause for concern.

III. Population Exposure to Water Trends

Water depletion also has more serious welfare implications if it affects more people. Figures 2c–d show the global population's exposure to water resource trends by overlaying trends in the GRACE data with gridded population estimates. The results show an extreme concentration of the global population in the parts of the world losing water most rapidly, along with a moderate concentration in regions gaining water. Over 1.3 billion people live in the most rapidly depleting decile of the world's arable land, nearly three times as many as in deciles with stable water resources. The map shows that this pattern is driven largely by parts of northern India and northeastern China, some of the most densely populated locations on earth.

Encouragingly, employment in these rapidly depleting regions is not especially concentrated in agriculture, by far the most water-dependent sector of the economy. Using country-level data from the FAO, we calculate that the average agricultural employment share for grid cells in the bottom decile of ΔTWS is 24%, below the global average and far below the 36% share in grid cells gaining water fastest. Moreover, Appendix Figure A2 shows that the world's population is disproportionately concentrated in arable regions with more rainfall and shallow groundwater tables, suggesting population density correlates differentially with static versus dynamic measures of water availability.

IV. Agricultural Exposure to Water Trends

Given that the overwhelming majority of human water consumption occurs in agriculture, the welfare consequences of global depletion depend on the degree to which it is concentrated in especially agriculturally productive regions. To investigate this, Figures 2e-f overlay trends in the GRACE data with gridded estimates of potential crop productivity from the FAO's Global Agro-Ecological Zones (GAEZ) database. We construct an aggregate index across the 38 crops in GAEZ that computes the z-score of each crop's productivity in each grid cell relative to the global distribution, and then takes the average across crops weighting by cropped area estimates from Monfreda, Ramankutty and Foley (2008) (see Appendix A.B for details).

The results in Figure 2f show a clear pattern in which the parts of the world losing water fastest have the lowest potential crop yields. The map shows that these relatively unproductive agricultural regions with rapid depletion include Iran, Saudi Arabia, Tibet, and northwestern China. Further, Appendix Figure A4 shows that a similar pattern of low productivity in depleting regions also holds for rice, but not for wheat, which are two of the most water-intensive staple crops. However, potential productivity and realized production can differ substantially; we use gridded GAEZ estimates of actual production to calculate that the decile of most rapid water loss currently grows 19% of global cereal tonnage, suggesting that current production patterns may need to shift to address possible future water shortages (see Appendix Figure A7).

V. Water Scarcity and Virtual Water Trade

The consequences of the evolving local water scarcity documented above are likely to depend critically on the degree to which water can be sourced from abroad. Although water itself is rarely traded because of its low value-to-weight ratio, its service as a factor of agricultural production can be exchanged indirectly through trade in agricultural goods. The scientific literature typically refers to this as "virtual water trade" following Allan (1998).

Figure 3a maps country-level net virtual water imports from crops and crop-derived food commodities in 2009. Most of Africa and the Middle East are net importers of virtual water, but the largest net importers are concentrated in East Asia (China, Japan, South Korea) and Central Europe (the Netherlands, Germany, Italy). The largest net exporters are the U.S. and Brazil, both major agricultural producers, followed by other large producers in the Americas (Argentina and Canada) and South Asia (India).

In the driest regions, virtual water imports seem to play an indispensable role in offsetting local water scarcity. Figure 3b shows that, on average, regions with the lowest rainfall rely most

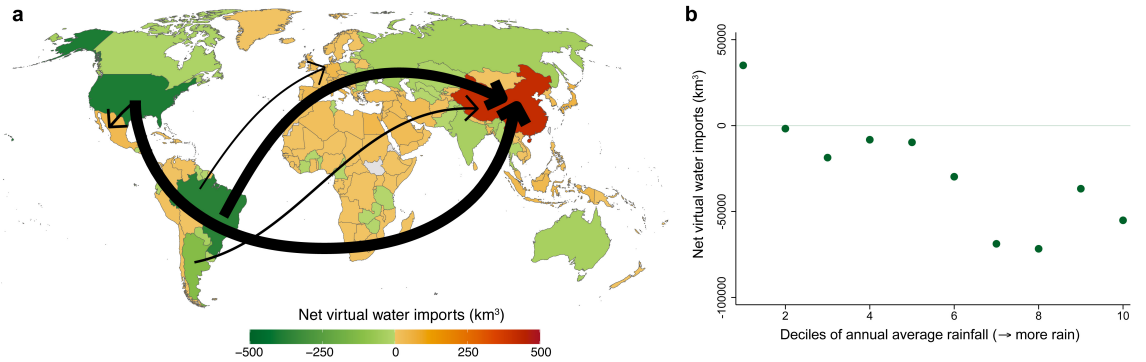

FIGURE 3. GLOBAL VIRTUAL TRADE IN AGRICULTURAL WATER

Note: Map colors in **a** show estimates of imports minus exports of agricultural "virtual water", or water consumed in the production process of agricultural goods. Positive values indicate imports of water embedded in traded agricultural goods that exceed exports. The five largest bidirectional flows are shown with arrows, where arrow width indicates flow magnitude. Plot in **b** shows average net virtual water imports for each decile of annual average rainfall over arable lands.

on imports for their water-intensive consumption. But, in general, water does not necessarily flow from water-abundant to water-scarce regions. Differences in relative agricultural productivity and relative arable land endowments can cause virtual water to flow from scarce regions to abundant ones. How exactly trade can exacerbate or mitigate these regional inequities in water resources is an important topic we study in Carleton, Crews and Nath (2023).

REFERENCES

Allan, John A. 1998. "Virtual water: A strategic resource." *Ground water*, 36(4): 545–547.

Carleton, Tamma, Levi Crews, and Ishan Nath. 2023. "Agriculture, trade, and the spatial efficiency of global water use."

Chen, JL, CR Wilson, and BD Tapley. 2013. "Contribution of ice sheet and mountain glacier melt to recent sea level rise." *Nature Geoscience*, 6(7): 549–552.

Dalin, Carole, Yoshihide Wada, Thomas Kastner, and Michael J. Puma. 2017. "Groundwater depletion embedded in international food trade." *Nature*, 543(7647): 700–704.

Fan, Y., H. Li, and G. Miguez-Macho. 2013. "Global patterns of groundwater table depth." *Science*, 339(6122): 940–943.

Gleick, Peter H, and Heather Cooley. 2021. "Freshwater scarcity." *Annual Review of Environment and Resources*, 46: 319–348.

Mekonnen, M. M., and A. Y. Hoekstra. 2011. "The green, blue and grey water footprint of crops and derived crop products." *Hydrology and Earth System Sciences*, 15(5): 1577–1600.

Monfreda, Chad, Navin Ramankutty, and Jonathan A. Foley. 2008. "Farming the planet: Geographic distribution of crop areas, yields, physiological types, and net primary production in the year 2000." *Global Biogeochemical Cycles*, 22(1).

Rodell, M., J. S. Famiglietti, D. N. Wiese, J. T. Reager, H. K. Beaudoing, F. W. Landerer, and M.-H. Lo. 2018. "Emerging trends in global freshwater availability." *Nature*, 557(7707): 651–659.

Tapley, Byron D, Michael M Watkins, Frank Flechtner, Christoph Reigber, Srinivas Bettadpur, Matthew Rodell, Ingo Sasgen, James S Famiglietti, Felix W Landerer, Don P Chambers, et al. 2019. "Contributions of GRACE to understanding climate change." *Nature climate change*, 9(5): 358–369.

Tapley, Byron D., Srinivas Bettadpur, John C. Ries, Paul F. Thompson, and Michael M. Watkins. 2004. "GRACE measurements of

mass variability in the earth system." *Science*, 305(5683): 503–505.

ONLINE APPENDIX

A. Data

GRAVITY RECOVERY AND CLIMATE EXPERIMENT

The Gravity Recovery and Climate Experiment (GRACE) satellite mission was launched in 2002 by the U.S. National Aeronautics and Space Administration (NASA) and the German Deutsche Forschungsanstalt für Luft und Raumfahrt (DLR). A "follow-on" mission to extend the satellite record was launched in 2018 and is ongoing. GRACE missions are composed of two identical spacecraft, flying 220 km apart in the same orbital plane about 500 km above the Earth. The missions are designed to measure changes in Earth's gravitational pull. As the pair passes over regions on Earth's surface with greater mass, they will face stronger gravitational pull, affecting the distance between the lead and trailing satellites. Instruments on board generate precise measurements of the changing distance between the two satellites while in orbit, accurate up to one micrometer (μm) per second Tapley et al. (2004).

Because water moves in large quantities through the hydrologic cycle at a rate far faster than other processes that move mass across the Earth's surface, mass variations uncovered by GRACE are mostly attributable to changes in water content as it cycles between ocean, atmosphere, continents, glaciers, and polar ice caps (Tapley et al., 2004). This monthly output has been used to study ocean currents (Wahr, Jayne and Bryan, 2002), measure ground water storage on land (Rodell, Velicogna and Famiglietti, 2009), and document exchanges between ice sheets or glaciers and the oceans (Jacob et al., 2012), among many other applications. GRACE "solutions" of these monthly data – a solution converts distances between satellites into estimates of changing mass – are available in gridded form across the globe. We use the Goddard Space Flight Center (GSFC) mass concentration solution RL06v2.0, which converts time-variable gravity into centimeters of equivalent water height for 41,168 equal-area blocks, called mascons, which measure $1^\circ \times 1^\circ$ ($\sim$ 111.11km$\times$111.11km) at the equator (Loomis, Luthcke and Sabaka, 2019).

Following extensive scientific literature (e.g., Rodell, Velicogna and Famiglietti (2009); Richey et al. (2015); Rodell et al. (2018)), we assume that changes in mass recovered by GRACE can be treated as changes in total water storage (ΔTWS), which is composed of the following elements:

$$\Delta TWS = \Delta groundwater + \Delta surface\ water + \Delta soil\ moisture + \Delta snow\ water\ equivalent \tag{A1}$$

Throughout our analysis, we abstract from any decomposition of ΔTWS and directly use this aggregate measure of water storage.

GRACE has the important advantage of providing global-scale estimates of changes in total water availability; no other data product comes close to presenting such a comprehensive picture of changing water resources. However, like all remotely sensed data, there are many important limitations of the data. First, all changes in Earth's gravitational field are recovered in GRACE, not only those due to changing water resources. For example, large landslides, mass human migrations, and large-scale mining activities, among other factors, can plausibly drive variation in gravitational pull. In our analyses, all of these changes are interpreted as changes in water resources. While this may appear limiting, prior research has documented that water dominates the overall variation in GRACE (Tapley et al., 2004), and that land surface and/or hydrologic models that are used to isolate specific components of GRACE (e.g., ground water) are highly sensitive to difficult-to-calibrate model parameters (Long et al., 2013). We therefore follow a large literature in interpreting gravitational anomalies from GRACE as changes in water resources and analyzing only aggregate TWS measures.

Second, the relatively low spatial resolution of GRACE ($1^\circ \times 1^\circ$) makes it valuable for global-scale analysis, but of limited use for many local water resource management questions. Other remotely sensed datasets, such as OpenET for measuring evapotranspiration (Melton et al., 2022) or InSAR for measuring recharge (Neely et al., 2021), are available in some regions of the world and are undoubtedly more appropriate for certain applications.

Finally, GRACE gives a measure of changes in water storage, but not estimates of available water stocks. Changes in gravitational pull are estimated from GRACE by taking a residual relative to a modeled estimate of the geoid – the hypothetical shape of the Earth. The data are represented as *anomalies* in the average gravitational field, which prohibits any interpretation of output in levels. Moreover, because this method relies heavily on the modeled geoid, there is undoubtedly measurement error that may influence downstream empirical estimation (Proctor, Carleton and Sum, 2023).

B. Methods

Virtual Water Trade

We follow a standard approach to computing virtual water trade (d'Odorico et al., 2019). The virtual water trade for a single product k from a given country i to another country j, VWT_{ij}^k (m^3), is the product of the virtual water content of product k produced in country i, VWC_i^k (m^3/tonne), and the trade flow of crop k from i to j, Q_{ij}^k (tonnes). A country's net virtual water imports are then simply $\text{nVWI}_i = \sum_k \sum_j (\text{VWT}_{ji}^k - \text{VWT}_{ij}^k)$.

Data on trade flows for the year 2009 come from UN Comtrade. Products are defined at the HS6 level. We restrict our attention to crops and crop-derived food commodities. Country-specific estimates of virtual water content for each crop and crop-derived food commodity come from Mekonnen and Hoekstra (2011). These are calculated as the average ratio between total crop evapotranspiration in the growing season and annual crop yield over the years 1996–2005. We consider only the green and blue water content for each crop and commodity.[2]

In total, our sample includes 228 distinct HS6 codes with non-zero virtual water flows in 2009. The top fifteen crops by virtual water flows—mostly cereals, oilseeds, and cotton lint—account for almost exactly 80% of the total volume.

C. Figures

[2]Green water is precipitation water directlycontributing to the soil water balance in the crops' root zone in the absence of irrigation. Blue water is irrigation water withdrawn from surface water bodies and aquifers. Mekonnen and Hoekstra (2011) also provide estimates inclusive of grey water, which is the water volume required to dilute pollutants to a concentration that meets a given country's water quality standards. Including grey water does not qualitatively change our results.

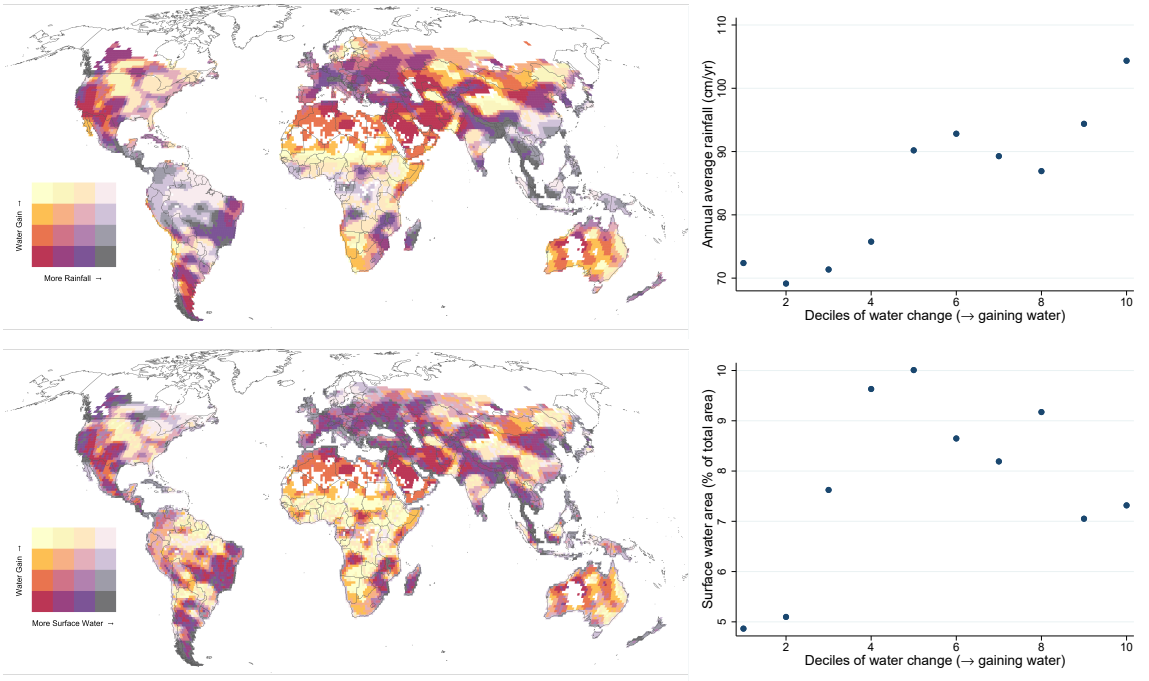

FIGURE A1. WATER LOSS AND BASELINE WATER AVAILABILITY

Note: Top panel: Map shows trends in total water storage (centimeters of equivalent water height per year) against average annual rainfall (centimeters per year). Plot shows average annual rainfall for each decile of trends in total water storage across global arable lands. Bottom panel: Map shows trends in total water storage against presence of surface water (percent of grid cell covered with surface water), derived from satellite-based estimates from (Pekel et al., 2016). Plot shows average surface water area for each decile of trends in total water storage across global arable lands.

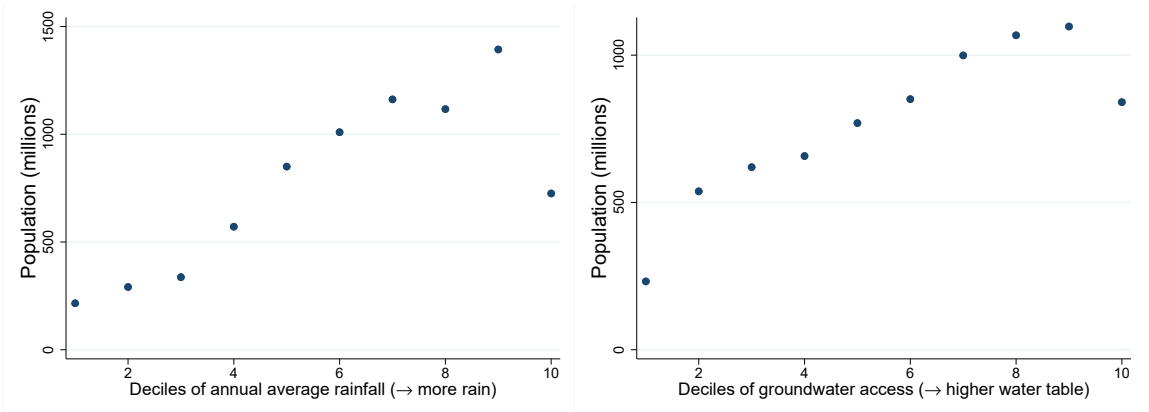

FIGURE A2. POPULATION EXPOSURE TO RAINFALL AND GROUNDWATER TABLE DEPTH

Note: Left panel plots the total population on arable land in each decile of the world's distribution of annual average rainfall. Right panel plots the total population on arable land in each decile of the world's groundwater table depth.

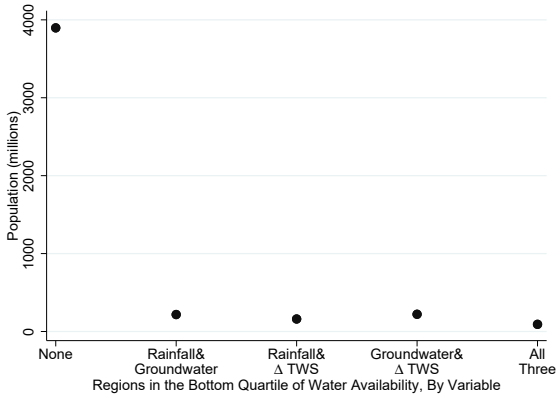

FIGURE A3. POPULATION EXPOSURE TO MULTIPLE SOURCES OF WATER STRESS

Note: Figure shows the total population over arable lands within grid cells that fall into zero, one, two, or three of the following water stress categories: (i) lowest quartile of total water storage trends; (ii) lowest quartile of average annual rainfall; (iii) lowest quartile of depth to groundwater.

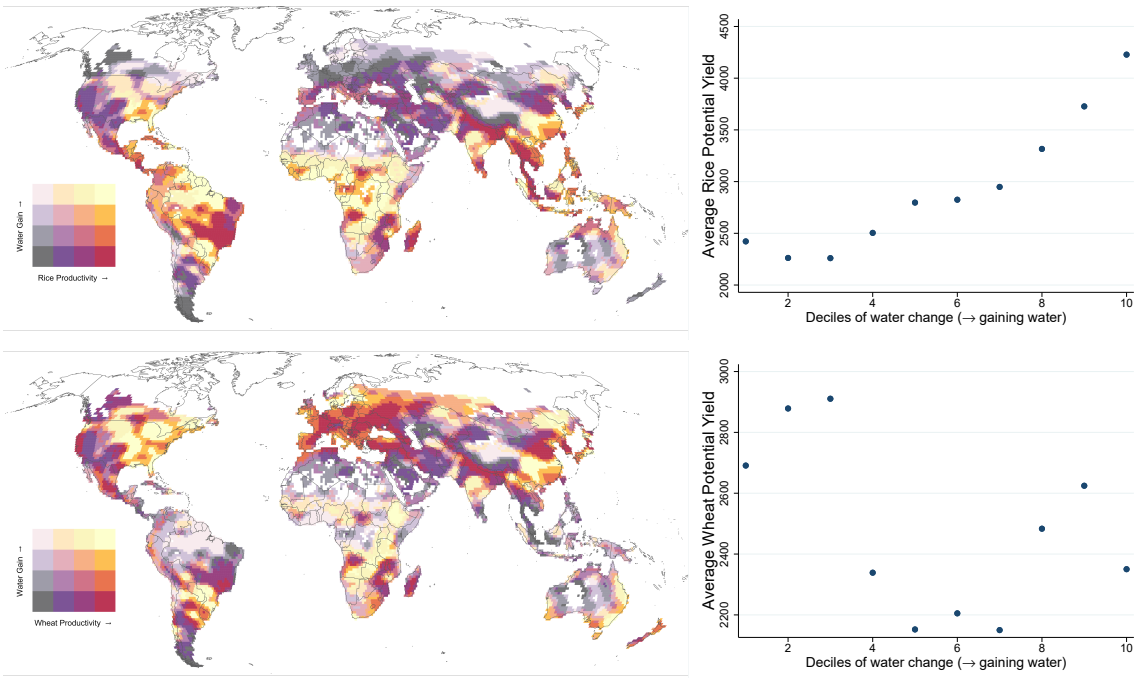

FIGURE A4. TOTAL WATER STORAGE TRENDS AND AGRICULTURAL PRODUCTIVITY: RICE AND WHEAT

Note: Top panel: Map shows trends in total water storage (centimeters of equivalent water height per year) against potential productivity of rice from GAEZ (tons/acre). Plot shows average rice potential yield in each decile of trends in total water storage across global arable lands. Bottom panel: Map shows trends in total water storage against potential productivity of wheat from GAEZ (tons/acre). Plot shows average wheat potential yield in each decile of trends in total water storage across global arable lands.

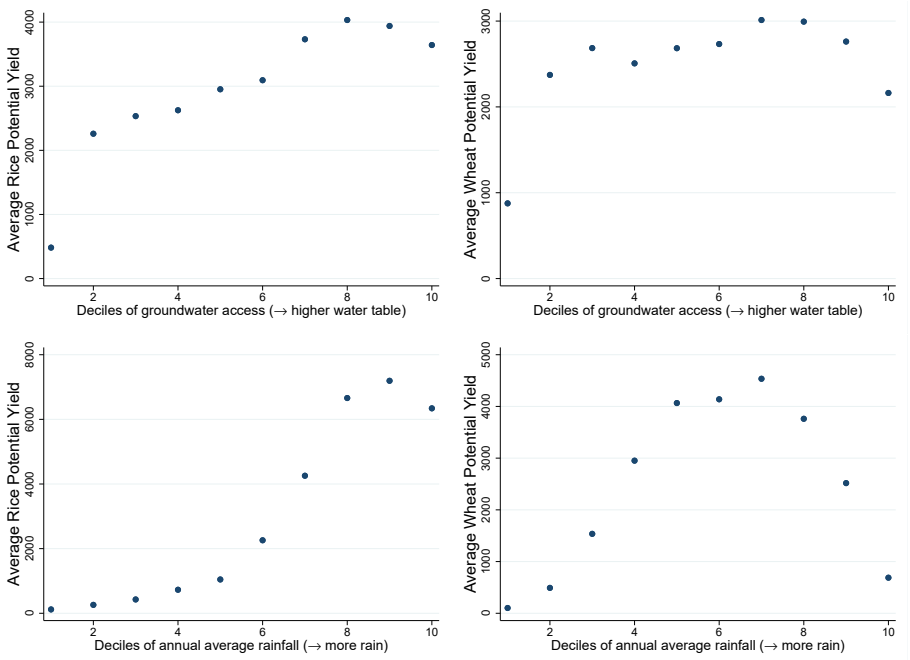

FIGURE A5. WATER STRESS AND AGRICULTURAL PRODUCTIVITY: RICE AND WHEAT

Note: Scatter plots show the average potential yield for rice (left column) and wheat (right column) in each decile of the global distribution of depth to groundwater (top row) and average annual rainfall (bottom row) over arable lands.

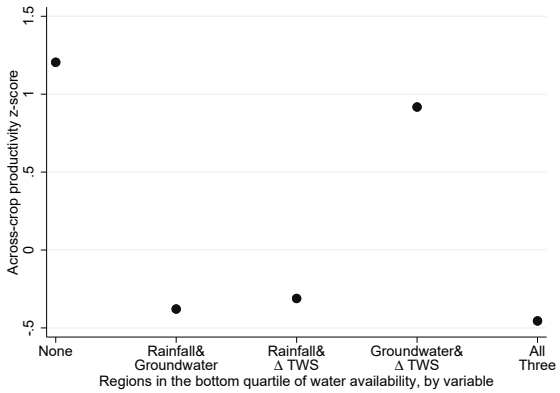

FIGURE A6. AGRICULTURAL PRODUCTIVITY IN REGIONS FACING MULTIPLE SOURCES OF WATER STRESS

Note: Figure shows the average across-crop potential agricultural productivity over arable lands within grid cells that fall into zero, one, two, or three of the following water stress categories: (i) lowest quartile of total water storage trends; (ii) lowest quartile of average annual rainfall; (iii) lowest quartile of depth to groundwater. Productivity z-scores are estimated by averaging 38 crop-specific agronomic yield estimates from GAEZ using cropped area weights from Monfreda, Ramankutty and Foley (2008) (see main text for details).

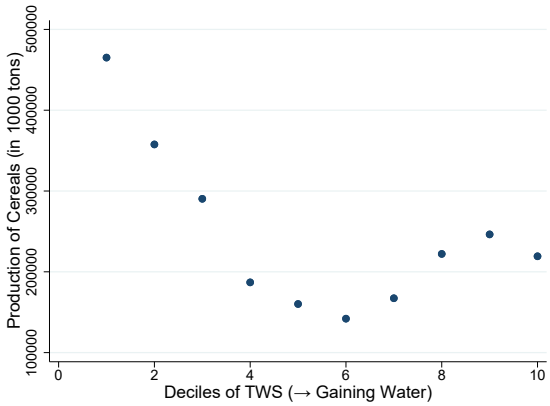

FIGURE A7. TOTAL WATER STORAGE TRENDS AND REALIZED CEREAL PRODUCTION

Note: Plot shows total quantity of cereal production in each decile of the global distribution of trends in total water storage. Cereal production is calculated using gridded estimates of realized production of wheat, rice, maize, sorghum, millet, barley, and "other cereals" from GAEZ.

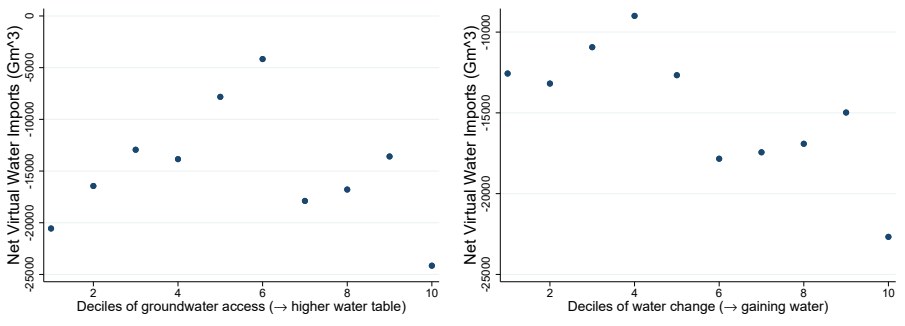

FIGURE A8. VIRTUAL WATER IMPORTS, GROUNDWATER TABLE DEPTH, AND TRENDS IN TOTAL WATER STORAGE

Note: Scatter plots show average net virtual water imports in each decile of the global distribution of depth to groundwater (left) and trends in total water storage (right). Both hydrological measures have been aggregated over the arable lands within each country before deciles are computed.

*

REFERENCES

d'Odorico, Paolo, Joel Carr, Carole Dalin, Jampel Dell'Angelo, Megan Konar, Francesco Laio, Luca Ridolfi, Lorenzo Rosa, Samir Suweis, Stefania Tamea, and Marta Tuninetti. 2019. "Global virtual water trade and the hydrological cycle: Patterns, drivers, and socio-environmental impacts." *Environmental Research Letters*, 14(5).

Jacob, Thomas, John Wahr, W Tad Pfeffer, and Sean Swenson. 2012. "Recent contributions of glaciers and ice caps to sea level rise." *Nature*, 482(7386): 514–518.

Long, Di, Bridget R. Scanlon, Laurent Longuevergne, Alexander Y. Sun, D. Nelun Fernando, and Himanshu Save. 2013. "GRACE satellite monitoring of large depletion in water storage in response to the 2011 drought in Texas." *Geophysical Research Letters*, 40(13): 3395–3401.

Loomis, BD, SB Luthcke, and TJ Sabaka. 2019. "Regularization and error characterization of GRACE mascons." *Journal of geodesy*, 93: 1381–1398.

Mekonnen, M. M., and A. Y. Hoekstra. 2011. "The green, blue and grey water footprint of crops and derived crop products." *Hydrology and Earth System Sciences*, 15(5): 1577–1600.

Melton, Forrest S, Justin Huntington, Robyn Grimm, Jamie Herring, Maurice Hall, Dana Rollison, Tyler Erickson, Richard Allen, Martha Anderson, Joshua B Fisher, et al. 2022. "OpenET: Filling a critical data gap in water management for the western United States." *JAWRA Journal of the American Water Resources Association*, 58(6): 971–994.

Monfreda, Chad, Navin Ramankutty, and Jonathan A. Foley. 2008. "Farming the planet: Geographic distribution of crop areas, yields, physiological types, and net primary production in the year 2000." *Global Biogeochemical Cycles*, 22(1).

Neely, Wesley R, Adrian A Borsa, Jennifer A Burney, Morgan C Levy, Francesca Silverii, and Michelle Sneed. 2021. "Characterization of groundwater recharge and flow in California's San Joaquin Valley from InSAR-observed surface deformation." *Water resources research*, 57(4): e2020WR028451.

Pekel, Jean-François, Andrew Cottam, Noel Gorelick, and Alan S. Belward. 2016. "High-resolution mapping of global surface water and its long-term changes." *Nature*, 540: 418–422.

Proctor, Jonathan, Tamma Carleton, and Sandy Sum. 2023. "Parameter recovery using remotely sensed variables." National Bureau of Economic Research.

Richey, Alexandra S., Brian F. Thomas, Min-Hui Lo, John T. Reager, James S. Famiglietti, Katalyn Voss, Sean Swenson, and Matthew Rodell. 2015. "Quantifying renewable groundwater stress with GRACE." *Water Resources Research*, 51(7): 5217–5238.

Rodell, Matthew, Isabella Velicogna, and James S. Famiglietti. 2009. "Satellite-based estimates of groundwater depletion in India." *Nature*, 460(7258): 999–1002.

Rodell, M., J. S. Famiglietti, D. N. Wiese, J. T. Reager, H. K. Beaudoing, F. W. Landerer, and M.-H. Lo. 2018. "Emerging trends in global freshwater availability." *Nature*, 557(7707): 651–659.

Tapley, Byron D., Srinivas Bettadpur, John C. Ries, Paul F. Thompson, and Michael M. Watkins. 2004. "GRACE measurements of mass variability in the earth system." *Science*, 305(5683): 503–505.

Wahr, John M, Steven R Jayne, and Frank O Bryan. 2002. "A method of inferring changes in deep ocean currents from satellite measurements of time-variable gravity." *Journal of Geophysical Research: Oceans*, 107(C12).